ISA Transactions ■ (■■■■) ■■■–■■■

Contents lists available at ScienceDirect

ISA Transactions

journal homepage: www.elsevier.com/locate/isatrans

A hybrid disturbance rejection control solution for variable valve timing system of gasoline engines

Hui Xie *, Kang Song, Yu He

State Key Laboratory of Engines, Tianjin University, Weijin Road 92, Nankai District, Tianjin 300072, PR China

ARTICLE INFO

Article history:
Received 10 May 2013
Received in revised form
12 October 2013
Accepted 17 October 2013
This paper was recommended for publication by Jeff Pieper

Keywords:
Variable valve timing control
Active disturbance rejection control
Feed-forward control

ABSTRACT

A novel solution for electro-hydraulic variable valve timing (VVT) system of gasoline engines is proposed, based on the concept of active disturbance rejection control (ADRC). Disturbances, such as oil pressure and engine speed variations, are all estimated and mitigated in real-time. A feed-forward controller was added to enhance the performance of the system based on a simple and static first principle model, forming a hybrid disturbance rejection control (HDRC) strategy. HDRC was validated by experimentation and compared with an existing manually tuned proportional-integral (PI) controller. The results show that HDRC provided a faster response and better tolerance of engine speed and oil pressure variations.

1. Introduction

Timing for the opening and closing of valves in gasoline engines, determined by the relative angle of the crankshaft and camshaft, is essential for the gas exchange process. For optimal fuel efficiency and engine performance, valve timing must vary as engine rotational speed varies. The traditional fixed valve timing system is unable to provide appropriate matching between the valve train and the engine at different operation conditions. This phenomenon leads to unwanted pumping loss, resulting in deteriorated fuel economy. To alleviate this problem, electro-hydraulic variable valve timing (VVT) optimizes the gas-exchange process providing about 3–5% fuel-saving potential for traditional spark-ignited (SI) gasoline engines [1]. Further improvements to fuel economy can be achieved if homogenous charge compression ignition (HCCI), a new concept in combustion, can be realized by VVT, reducing the amount of pumping loss caused by low intake manifold pressure [2]. To improve SI combustion and make HCCI realizable, the valve timing fluctuation should be $\pm 1^\circ$ in crankshaft angle (°CA) [3] even in the face of disturbances such as speed and oil pressure variations.

Electro-hydraulic VVT is challenging to control because of the low sampling rate which is limited by the engine speed. A pair of position sensors, one for the crankshaft and one for the camshaft, measures the valve timing when the engine runs. Constrained by the practical sensors in production engines, the valve timing can only be fed back between one and eight times per engine cycle. Thus, the resulting sample rate can fall below 5 Hz at low engine speed, and varies with engine speed. Also challenging to control are the strong disturbances that exist in the VVT system in production engines, which are difficult to measure or model. The pressure difference between two oil chambers, supplied by the crankshaft driven oil pump, results in an engine speed-related driven force. Although the pressure difference can be controlled by a proportional solenoid, the response varies with the battery voltage leading to a time-variant actuator dynamic. Likewise, the frequent inverse force from the valve spring significantly disturbs valve timing [4]. The time delay and nonlinear characteristics of the hydraulic system also present control challenges to VVT control.

Various solutions to the aforementioned problems have been reported for VVT control. To deal with the disturbance from oil pressure variation caused by engine speed fluctuation, gain-scheduling PID according to engine speed is investigated. However, it was found that there are times, such as when the oil temperature is low, when the engine is cold, slow response or oscillation could take place [5] using this solution. This is because the oil flow resistance varies with oil temperature, changing the oil pressure difference inside the cam phaser, i.e., the driving force of valve timing. Consequently, the controller gain becomes inappropriate under varied system dynamics. To compensate for this influence from oil temperature, an estimation algorithm for pressure difference inside the cam phaser is designed, based on which PID gain-scheduling is adopted. However, utilizing this algorithm, the controller stability could be poor in steady state

* Corresponding author. Tel./fax: +86 22 27406842 8009,
Mobile: +86 13001344531.
E-mail addresses: xiehui@tju.edu.cn (H. Xie), songkangtju@tju.edu.cn (K. Song), Heyu@tju.edu.cn (Y. He).

0019-0578/$ - see front matter © 2013 ISA. Published by Elsevier Ltd. All rights reserved.
http://dx.doi.org/10.1016/j.isatra.2013.10.006

Nomenclature

ADRC	active disturbance rejection control
A_p	the effective sectional area of the piston in the solenoid
B_p	the viscous damping coefficient of the piston
b_0	the static gain in the ADRC canonical form
C_{ep}	the leakage coefficient of the crevice between the piston connection rod and the chamber
C_{ip}	the leakage coefficient of the crevice between the piston and the chamber
$DuCy_{Driving}$	driving-stage signal duty cycle
$DuCy_{Holding}$	the holding-stage duty cycle
ECU	engine control unit
FF	feed-forward
F_{Load}	the external force from the valve
f	disturbances in ADRC canonical form
$HDRC$	hybrid disturbance rejection control
$HCCI$	homogenous charge compression ignition
$ITAE$	integral time absolute error
K_p	the proportion gain in the proportion controller
K_{direct}	VVT timing driving direction factor based on ADRC and FF, −1 or 1, −1 for 100% duty cycle and 1 for 0% duty cycle
K_{direct_ADRC}	VVT timing driving direction factor based on ADRC, −1 or 1, −1 for 100% duty cycle and 1 for 0% duty cycle
K_{direct_FF}	VVT timing driving direction factor based on FF, −1 or 1, −1 for 100% duty cycle and 1 for 0% duty cycle
K_p	the gain between the solenoid position and PWM driving signal duty cycle
K_s	the stiffness of the spring
$LESO$	a linear extended state observer
m_t	the equivalent mass of the engine piston and valve
P_1	the oil pressure in the high pressure oil chamber
P_2	the oil pressure in the low pressure oil chamber
P_a	the atmospheric pressure
P_s	the oil pressure at the outlet port of the oil pump
PID	proportional-integral-differential control
PI	proportional-integral control
POG	power-oriented graphs model
PWM	pulse-width modulation
Q_1	the oil mass flow into the oil chamber
Q_2	the oil mass flow out of the oil chamber
Q_L	the oil mass flow rate through the solenoid inlet valve
SI	spark-ignited
$SISO$	single-input single-output
$T_{driving}$	the time duration of the driving-stage signal
T_{Cycle}	the time duration of one engine cycle
u	the PWM duty cycle for solenoid driving
u_m	the holding-stage duty cycle around 50
V_1	the high pressure oil chamber volume in the hydraulic cylinder
V_2	the low pressure oil chamber volume in the hydraulic cylinder
VVT	variable valve timing
W	the perimeter of the inlet valve
X_v	the solenoid position (ranging from −1 to 1)
x_p	the piston displacement of the cam phaser
α	a constant around 1, used to tune the weight of the feed-forward controller
β_ε	the oil effective volumetric modulus of elasticity
ρ	the oil density
ε	a constant, the oil pressure in the high pressure oil chamber divided by the oil pressure at the outlet port of the oil pump
v	the piston moving speed of the cam phaser
w_e	the external disturbance
ω_c	the controller bandwidth
ω_o	the observer bandwidth
θ_{fluct}	the fluctuation amplitude of valve timing at steady operating condition

condition if the controller gain is set very large to improve the response in the transient state [6]. Accordingly, a PID gain-switching solution based on steady and transient state detection is proposed [6]. Although these kinds of controllers can compensate for the disturbances, such as the engine speed, oil pressure, as well as oil temperature, they usually require time-consuming parameter optimization. Another possible choice is to use feed-forward control based on various kinds of models such as the neural network model [7], the discrete nonlinear model [8], and the power-oriented graphs (POG) model [9]. However, these models are usually too complex for an engine control unit (ECU) application due to the computational burden upon the processor.

To summarize, the dilemma is between the strong disturbances, the low sampling rate, and the limited disturbance rejection ability of existing PI controllers. Gain-scheduling PI control and dynamic model based feed-forward control can alleviate the dilemma, but suffer from time-consuming parameter optimization limiting their appeal for practical application.

In this paper, a new solution is presented based on the active disturbance rejection control (ADRC) concept [10–13] that has been widely used in many fields [14–16]. The engine speed, oil pressure, and battery voltage fluctuations of the VVT system are all treated as disturbances and are observed and canceled in real-time. Applying the parameterization method in [17] allows for an easy and intuitive tuning process. However, the control performance was limited due to the limited bandwidth. Feed-forward control was found to be effective in improving ADRC performance [18]. Therefore, to speed up the system, a simple static first principle model of the VVT system was used to design a feed-forward controller forming a hybrid disturbance rejection control (HDRC) strategy. Experimental results of HDRC and an existing manually tuned PI controller were obtained to evaluate the effectiveness of HDRC for the VVT system.

This paper is organized as follows: The VVT operation principle is described in Section 2. The HDRC strategy is presented in Section 3. Experimental validations on the VVT test bed are given in Section 4, with concluding remarks in Section 5.

2. Basic principle of the electro-hydraulic VVT system

2.1. VVT structure

The VVT system in this study is a typical electro-hydraulic system as shown in Fig. 1. The cam phaser housing is connected with the crankshaft, while the rotor is connected with the camshaft. The relative angle between the two shafts, denoted as the valve timing, is determined by the relative position of the housing and the rotor. Between the housing and the rotor, there are two oil chambers. The oil pressure differences between the chambers can be used to control the valve timing, forward or backward.

Please cite this article as: Xie H, et al. A hybrid disturbance rejection control solution for variable valve timing system of gasoline engines. ISA Transactions (2013), http://dx.doi.org/10.1016/j.isatra.2013.10.006

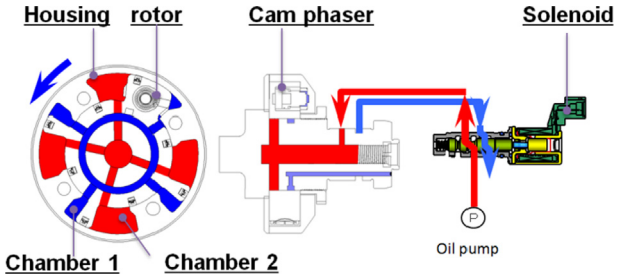

Fig. 1. Basic operating principle of electro-magnetic VVT system.

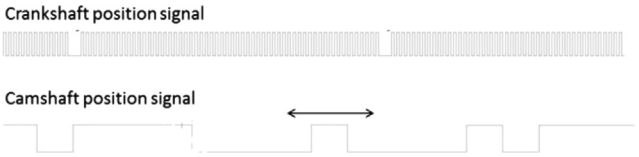

Fig. 2. Valve timing detection principle.

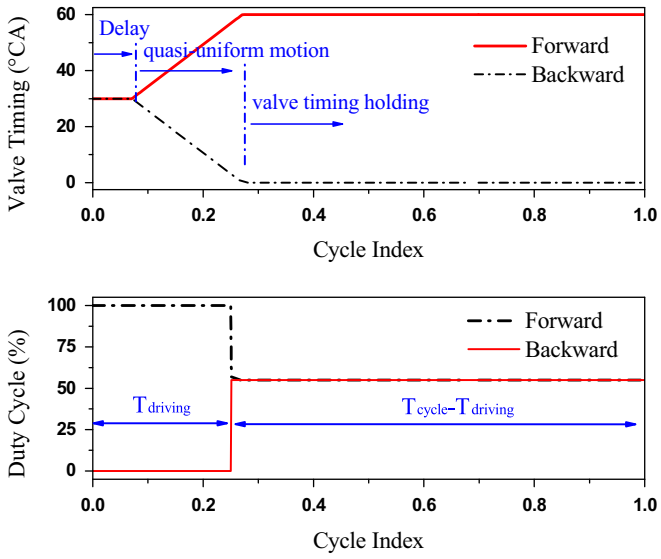

Fig. 3. Solenoid driving signal and the according response profile.

2.2. Valve timing detection

The camshaft and crankshaft position sensors are used for valve timing detection, producing the output signals for two complete revolutions as demonstrated by Fig. 2. The valve timing can then be calculated by analyzing the relative angle between the starting sequences of these two signals. Consequently, the sampling rate is limited between one and eight times per engine cycle. In this study, it is chosen to be once per engine cycle for simplicity.

2.3. Valve timing control

As mentioned in Section 2.1, the valve timing is controlled by the oil pressure difference between the housing and the rotor, which is adjusted by regulating the oil flow rate and direction by use of a proportional solenoid. The position of the proportional solenoid is controlled by a two-stage pulse-width modulation (PWM) signal (using 300 Hz frequency in this paper) as demonstrated in Fig. 3. The first stage is called driving-stage where the duty cycle of the signal is either 100% or 0% causing the core of the solenoid to beat one of its limits. In this condition, the oil flows into or out of the oil chamber, which can push or pull the rotor of the cam phaser to adjust the valve timing. The second stage is valve timing holding stage where the duty cycle is between 45% and 70% so the core of the solenoid is in the middle where almost no oil flows into or out of the cam phaser. In this condition, the valve timing can be partially maintained for a short period.

Accordingly, the typical response profile within one control cycle consists of three stages as demonstrated in Fig. 3 – delay, quasi-uniform motion, and valve timing holding. This response profile can be adjusted by the two-stage PWM signal through the adjustment of the driving-stage time fraction $T_{driving}/T_{Cycle}$, where $T_{driving}$ is the time duration of the driving-stage signal, T_{Cycle} is the time duration of one engine cycle and the holding-stage duty cycle. For example, the "quasi-uniform motion" stage extends with $T_{driving}/T_{Cycle}$ increasing, which could adjust the valve timing.

2.4. Experimental bench

The VVT test bench is shown in Fig. 4, and consisted of three parts – the simulation engine constructed by a cylinder head and a motor; the lubrication and valve timing driving system which included the oil pump, oil filter, oil heater, oil pressure regulating valve, and oil pipes; and the measurement and control system of an engine control unit (ECU), an industrial personal computer, the oil temperature and pressure sensor, position sensors (for crankshaft and camshaft), and a proportional solenoid. The VVT cam phaser is a self-developed electro-hydraulic one with the structure shown in Fig. 1. The engine speed, oil pressure, and temperature can all be flexibly controlled and measured on this platform. Experimental validation of HDRC was carried out on this platform, explained in detail in Section 4.

3. Controller synthesis

As has been analyzed, VVT system is typically a single-input single-output (SISO) system with low sampling rate, delay, and strong disturbances, such as like the fluctuation of oil pressure and temperature, battery voltage, and engine load as illustrated in Fig. 5. The goal of this study is to propose a practical solution for VVT control with fast response, high robustness and disturbance rejection ability, having parameters that are easy to tune without requirement for time-consuming gain-scheduling. The idea is to treat all the disturbances, varied system dynamics and external forces fluctuations, as a time-varying state "total disturbance", estimated and mitigated in real time by ADRC, assisted by feed-forward controller to enhance the response.

Therefore a new solution, HDRC, is proposed and illustrated in Fig. 6. The two-stage PWM signal (shown in Fig. 3), driving-stage and holding-stage, is synthesized by the "Signal synthesis" module which takes the engine speed into account, for the purpose of calculating the time duration of one engine cycle T_{Cycle}. The driving-stage signal, determined by ADRC and FF together, is defined by three parameters – valve timing adjusting direction factor (K_{direct}), driving-stage signal time duration ($T_{driving}$) and T_{cycle}, in which K_{direct}, a constant equals -1 or 1, determines the duty cycle (-1 for 0% duty cycle and 1 for 100% duty cycle), and $T_{driving}/T_{Cycle}$ defines the signal time fraction of one engine cycle ranging from 0 to 1. For the ADRC module, it treated all uncertainties inside the VVT system as total disturbance, estimated and mitigated in real time, producing the first part of the driving-stage signal parameters: $K_{direct\_ADRC} \times T_{driving\_ADRC}/T_{Cycle}$. However, due to the low sampling rate, the performance of ADRC is limited. Therefore, a static first principle model-based feed-forward (FF) controller was designed for the other part of driving-stage parameters $K_{direct\_FF} \times T_{driving\_FF}/T_{Cycle}$, in order to speed the system up.

Please cite this article as: Xie H, et al. A hybrid disturbance rejection control solution for variable valve timing system of gasoline engines. ISA Transactions (2013), http://dx.doi.org/10.1016/j.isatra.2013.10.006

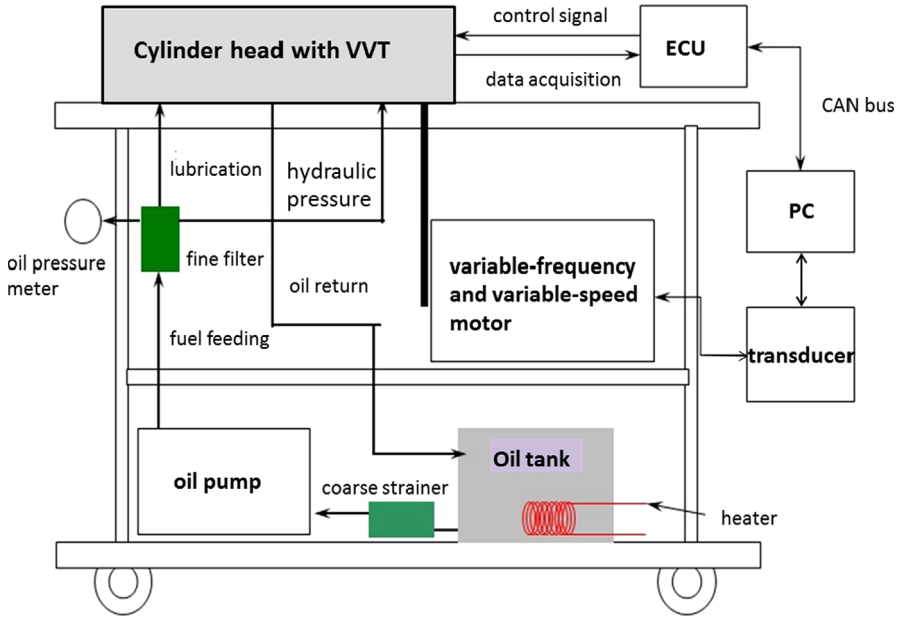

Fig. 4. Experimental bench configuration.

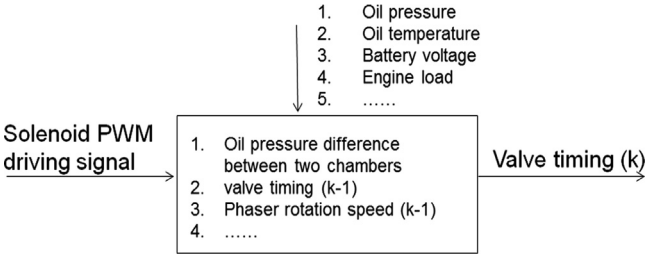

Fig. 5. Control problem description of VVT system.

In regards to the holding-stage signal, the time fraction has already been determined as $1-T_{driving}/T_{cycle}$, while its duty cycle is controlled by the holding-stage adjustment module, which will be described in detail in Section 3.3.

3.1. System modeling

In this study, the VVT system is approximated as an ideal system shown in Fig. 7, composing of a solenoid model and a linear hydraulic cylinder model with a spring and damper simulating the VVT cam phaser. The valve timing changing speed is approximated by the piston moving speed of the hydraulic cylinder in this model.

This solenoid position is assumed to be fully controlled by the PWM duty cycle

$$X_v = K_p(u-u_m) \tag{1}$$

where X_v is the solenoid position (ranging from -1 to 1), K_p is the gain between the solenoid position and PWM driving signal duty cycle, u is the PWM duty cycle (ranging from 0% to 100%), and u_m is the holding-stage duty cycle around 50%. $X_v>0$ indicates that the solenoid moves right and the inlet port (on the left in Fig. 8) is open.

The oil mass flow rate through the solenoid inlet valve Q_L can be estimated as follows:

$$Q_L = C_d \times W \times X_v\sqrt{(P_S-P_1)/\rho} \tag{2}$$

where C_d is the flow coefficient of the solenoid inlet valve, W is the perimeter of the inlet valve, P_s is the oil pressure at the outlet port of the oil pump, P_1 is the oil pressure in the high pressure oil chamber, and ρ is the oil density.

The oil mass flow rate into and out of the solenoid can also be estimated according to the continuity equation, supposing that the modulus of elasticity is constant, the oil pressure distribution is homogeneous, the leakage flow within the oil chamber and out of the chamber is laminar, and the pressure dynamic in the oil pipe between the solenoid and cam phaser can be neglected. Thus, the oil mass flow into and out of the oil chamber can be estimated as follows:

$$Q_1 = A_p\frac{dx_p}{dt}+C_{ip}(P_1-P_2)+C_{ep}P_1+\frac{V_1}{\beta_\varepsilon}\frac{dP_1}{dt} \tag{3}$$

$$Q_2 = A_p\frac{dx_p}{dt}+C_{ip}(P_1-P_2)-C_{ep}P_2+\frac{V_2}{\beta_\varepsilon}\frac{dP_2}{dt} \tag{4}$$

where Q_1 is the oil mass flow rate into the oil chamber through the solenoid inlet valve from the pump, A_p is the effective sectional area of the piston, x_p is the piston displacement, C_{ip} is the leakage coefficient of the crevice between the piston and the chamber, C_{ep} is the leakage coefficient of the crevice between the piston connection rod and the chamber, β_ε is the oil effective volumetric modulus of elasticity, and V_1 is the high pressure oil chamber volume. Q_2 is the oil mass flow rate out of the oil chamber, consisting of the oil through the solenoid inlet valve, leaked through the piston–cylinder liner crevice, and leaked outside the cylinder. P_2 is low pressure oil chamber pressure and V_2 is the low pressure oil chamber volume.

The two equations above are further simplified based on two assumptions. The oil is assumed to be incompressible (where $(V_1/\beta_\varepsilon)(dP_1/dt)=0$). Likewise, the internal leakage can be ignored when compared with the external one (so $C_{ip}(P_1-P_2)\ll C_{ep}P_1$, where P_2 is atmospheric pressure, $P_1=\varepsilon\times P_s$ with ε a constant, $Q_1\approx Q_L$). Therefore, the following equation can be obtained:

$$Q_L = A_p\frac{dx_p}{dt}+\epsilon\times C_{ep}\times P_S = A_p v+\epsilon C_{ep}P_S \tag{5}$$

where v is the moving speed of the piston.

Please cite this article as: Xie H, et al. A hybrid disturbance rejection control solution for variable valve timing system of gasoline engines. ISA Transactions (2013), http://dx.doi.org/10.1016/j.isatra.2013.10.006

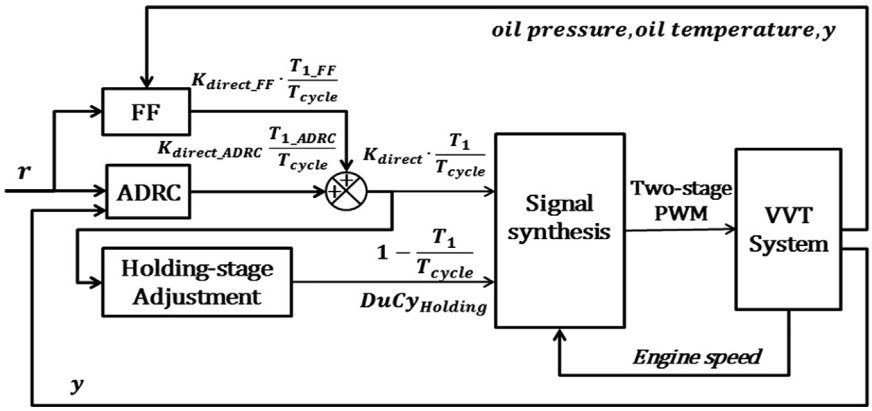

Fig. 6. Control structure of HDRC.

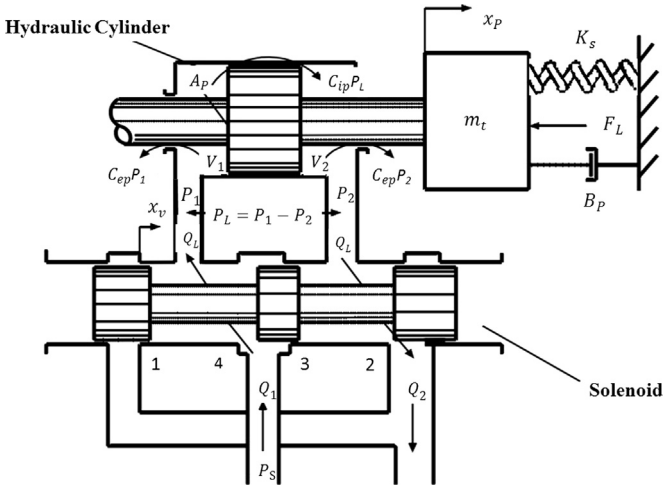

Fig. 7. Simplified model of the VVT system.

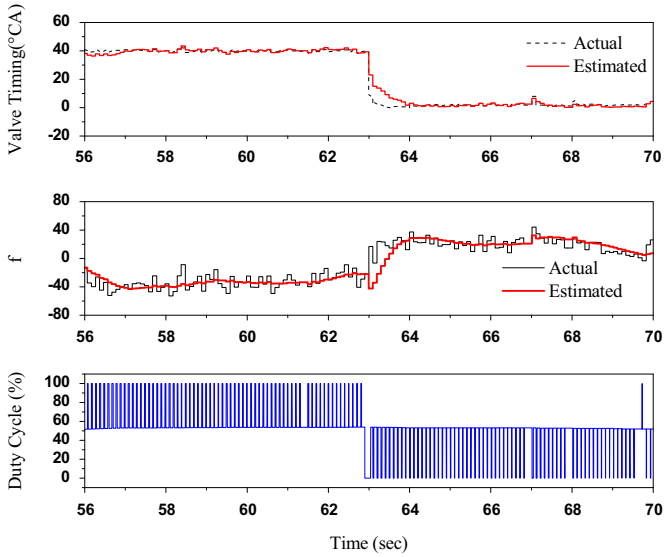

Fig. 8. LESO validation at 1200 rpm engine speed and 1.0 bar oil pressure.

The following equation can be made by analyzing the force produced by the oil pressure difference:

$$A_p(P_1-P_2)=m_t\frac{d^2x_p}{dt^2}+B_p\frac{dx_p}{dt}+K_Sx_p+F_{Load} \tag{6}$$

where m_t is the equivalent mass of the engine piston and valve, B_p is the viscous damping coefficient of the piston, K_s is the stiffness of the spring, and F_{Load} is the external force from the valve. The equation above can be approximated by

$$A_p(P_1-P_a)=F \tag{7}$$

where F is an equivalent force of all the right side elements in Eq. (6), and P_a is the atmospheric pressure.

Finally, the static model for the cam phaser motion speed estimation is achieved as follows:

$$v=\frac{K_pC_dW\sqrt{(P_S-(F/A_p)-P_a)/\rho}\times(u-u_m)-\epsilon C_{ep}P_S}{A_p} \tag{8}$$

where K_p, C_d, F, and C_{ep} can be estimated with a detailed simulation model [19]. W, P_s and A_p can be measured or calculated directly.

3.2. Active disturbance rejection control

Based on the model illustrated as Eq. (8) in Section 3.1, the VVT system can be approximated by a simple first order system as demonstrated in the following equation:

$$\begin{aligned}\upsilon=\dot{y}&=w_e+[K_pC_dW\sqrt{(P_s-F/A_p-P_a)/\rho}\times(u-u_m)-\epsilon C_{ep}P_s]/A_p\\&=w_e-[k_pC_dW\sqrt{(P_s-F/A_p-P_a)/\rho}\times u_m\\&\quad+\epsilon C_{ep}P_s]/A_p+k_pC_dW\sqrt{(P_s-F/A_p-P_a)/\rho}/A_pu\\&=w_e-[k_pC_dW\sqrt{(P_s-F/A_p-P_a)/\rho}\times u_m\\&\quad+\epsilon C_{ep}P_s]/A_p+[k_pC_dW\sqrt{(P_s-F/A_p-P_a)/\rho}/A_p-b_0]u+b_0u\\&=f+b_0u\end{aligned} \tag{9}$$

where y is the valve timing, υ is the moving speed of the piston (used to approximate the changing speed of the valve timing $\dot{y}$), w_e is the external disturbance, b_0 is an approximate value (49 is used in this paper) of $k_pC_dW\sqrt{(P_s-F/A_p-P_a)/\rho}/A_p$ at a fixed operating point (3.5 bar oil pressure, 40 °C oil temperature in this paper), and f is referred as the total disturbance as shown in the following equation:

$$\begin{aligned}f&=w_e-[k_pC_dW\sqrt{(P_s-F/A_p-P_a)/\rho}\times u_m+\epsilon C_{ep}P_s]/A_p\\&\quad+[k_pC_dW\sqrt{(P_s-F/A_p-P_a)/\rho}/A_p-b_0]\times u\end{aligned} \tag{10}$$

The idea of ADRC is to have f estimated and canceled; leaving an integral plant that can be easily controlled. To do so, we first

Please cite this article as: Xie H, et al. A hybrid disturbance rejection control solution for variable valve timing system of gasoline engines. ISA Transactions (2013), http://dx.doi.org/10.1016/j.isatra.2013.10.006

convert the differential equation into an extended state space form

$$\begin{cases} \dot{x}_1 = x_2 + b_0 u \\ \dot{x}_2 = h \\ y = x_1 \end{cases} \tag{11}$$

$$\begin{cases} \dot{x} = Ax + bu + Eh \\ y = Cx \end{cases} \tag{12}$$

with $x_2 = f$ added as an augmented state, $h = \dot{f}$ unknown, and $A = \begin{bmatrix} 0 & 1 \\ 0 & 0 \end{bmatrix}$, $B = \begin{bmatrix} b_0 \\ 0 \end{bmatrix}$, $C = [1 \quad 0]$, $E = \begin{bmatrix} 0 \\ 1 \end{bmatrix}$.

This allows the construction of a linear extended state observer (LESO) in the form of

$$\begin{cases} \dot{z} = Az + bu + L(y - \hat{y}) \\ y = Cz \end{cases} \tag{13}$$

with L being the observer gain vector and $z = [z_1, z_2]^T$ being the estimated states. In other words, z_2 is obtained in real-time as the approximation of f in Eq. (9), and the control law $u = (-z_2 + u_0)/b_0 = K_{direct\_ADRC} \times T_{driving\_ADRC}/T_{cycle}$ ranging from -1 to 1. Here K_{direct_ADRC} is a constant equals -1 or 1, representing the duty cycle of driving-stage signal, i.e., 0% duty cycle when negative, 100% duty cycle when positive, and $T_{driving\_ADRC}$ is the duration of the driving stage signal calculated from ADRC.

Thus, Eq. (9) approximately to $\dot{y} \approx u_0$ which can easily be controlled with a proportional controller

$$u_0 = K_p(r - z_1) \tag{14}$$

where r is the setpoint, K_p is the proportion gain, and z_1 is the estimation of x_1.

The observer gain and the P controller parameters can be easily tuned using the parameterization method in [17]. The tuning parameters include the observer bandwidth ω_o, the control bandwidth ω_c, and the physical constant b_0. For the VVT system, ω_o is chosen around 5 while ω_c ranged from about 0.5 to 2 at 1200 rpm engine speed with a sampling rate of 10 Hz (sampling every engine cycle, in the meanwhile the crankshaft turns two revolutions).

Finally, with the LESO tuned for an operation point of 1200 rpm and 3.5 bar oil pressure, the system was tested with the oil pressure at 1.0 bar (much lower than the normal level) to analyze the disturbance rejection ability of the controller. The result is illustrated in Fig. 8 with the actual disturbance $f = \dot{y} - b_0 u$. Both y and f are estimated but with a small amount of error, especially during the transient process. This has a close relationship with the low sampling rate (10 Hz at 1200 r/min engine speed), limiting its performance to some extent.

3.3. Feed-forward control

To speed the system up, a feed-forward controller was designed based on the simple static first principle model demonstrated in Eq. (8). The driving stage signal duty cycle and its time fraction in one engine cycle can be calculated by

$$K_{direct\_FF} \times \frac{T_{driving\_FF}}{Tcycle} = \alpha \times \frac{r - y}{vTcycle} \tag{15}$$

where K_{direct_FF} is a constant, -1 or 1, defining the desired VVT timing adjusting direction. That is, when K_{direct_FF} equals -1, the duty cycle of the driving-stage signal is 0%, and when K_{direct_FF} equals to 1, and the duty cycle should be 100%. $T_{driving\_FF}$ is the duration of the driving-stage signal calculated by FF, r is the desired valve timing, y is the actual valve timing, and α is a coefficient used to tune the weight of the feed-forward controller. The smaller α is the more conservatively the feed-forward controller is used. Here the delay period (the first stage of the output response in Fig. 3) is ignored for simplicity.

The feed-forward control is actually a gain-scheduled proportion control, as the proportion varies with the oil pressure, oil temperature, etc. Therefore, feed-forward control here is an effective improvement of ADRC in the transient process in the case of operating condition variations under limited sampling rate.

Finally, the FF controller is integrated with the ADRC controller. Thus, in the transient operating process (when the difference between y and r is over 5 °CA in this paper), the driving-stage signal becomes $K_{direct}T_{driving}/T_{Cycle} = K_{direct\_FF}T_{driving\_FF}/T_{Cycle} + K_{direct\_ADRC}T_{driving\_ADRC}/T_{Cycle}$. The duty cycle (0% or 100%) is determined by the sign of K_{direct}, a constant equals -1 or 1, i.e., 0% duty cycle is selected when K_{direct} equals -1 or 100% duty cycle when K_{direct} equals 1. The according time fraction of one engine cycle $T_{driving}/T_{cycle}$, ranging from 0?to 1, equals the absolute value of $K_{direct\_FF}T_{driving\_FF}/T_{Cycle} + K_{direct\_ADRC}T_{driving\_ADRC}/T_{Cycle}$.

The control performance comparison between the controllers with and without FF was demonstrated in Fig. 9. Here, the settling time is defined as the time duration between the moment when the valve timing order is sent and the moment after which the valve timing error stays within ± 5 °CA. It could be noticed that overshoot was reduced with the FF controller, resulting in shortened (about 39%) settling time defined above. It is because the low sampling rate leads to the LESO's slow tracking of both y and f,

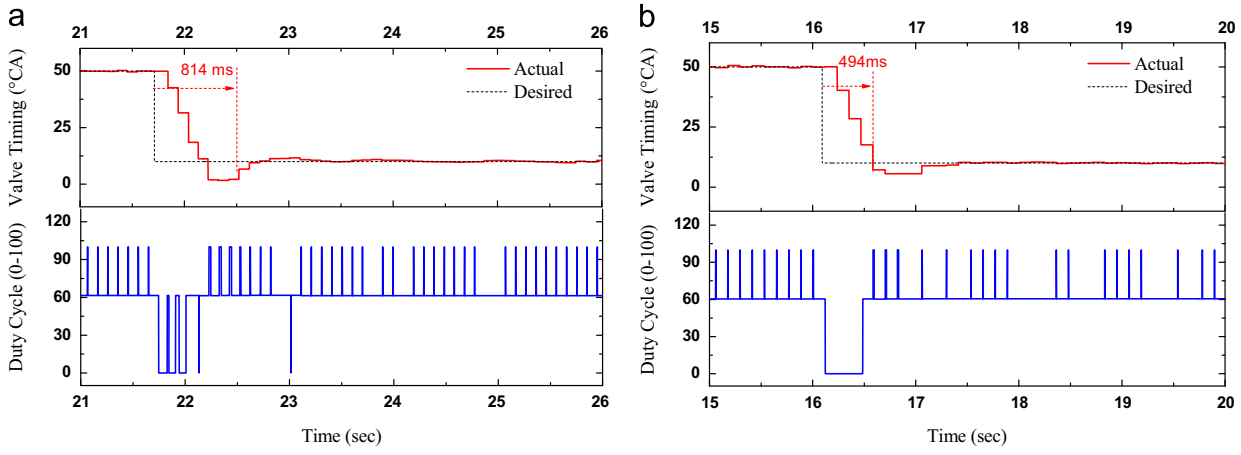

Fig. 9. Transient performance comparison with and without feed-forward control at 1200 rpm engine speed and 3.5 bar oil pressure. (a) without feed-forward control and (b) with feed-forward control.

Please cite this article as: Xie H, et al. A hybrid disturbance rejection control solution for variable valve timing system of gasoline engines. ISA Transactions (2013), http://dx.doi.org/10.1016/j.isatra.2013.10.006

making VVT timing overshoot when pursues short rising time. Fortunately, this conflict was alleviated by feed-forward control.

3.4. Holding-stage duty cycle adjustment

Since the holding-stage (as shown in Fig. 3) usually takes a much larger time fraction of one engine cycle, a small duty cycle error may lead to a large valve timing error, increasing the compensation burden of HDRC. Therefore, an online adjustment algorithm is needed to correct the holding-stage duty cycle $DuCy_{Holding}$ based on the observation of the driving-stage duty cycle $DuCy_{Driving}$ and the valve timing error Δy

$$HoldingCyl_{cor} = \frac{DuCy_{Driving} - DuCy_{Holding}}{\alpha(1+\beta\Delta y)} \tag{16}$$

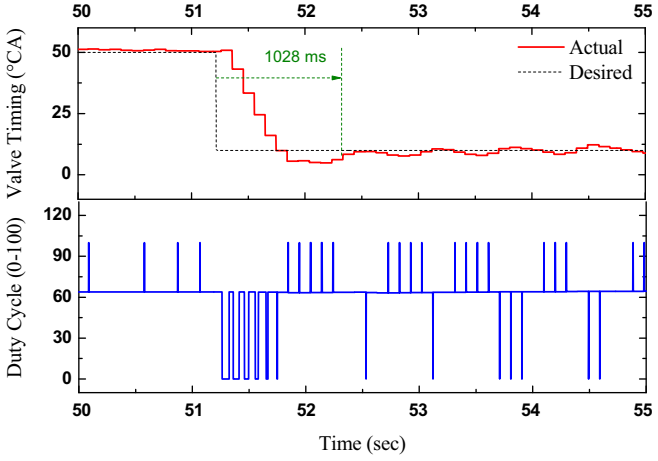

Fig. 10. 50–10 °CA step test of PI at 1200 rpm engine speed and 3.5 bar oil pressure.

Table 1
Control performance comparison between PI, ADRC and HDRC at 1200 r/min and 3.5 bar oil pressure.

	T_s (ms)	*ITAE* (°CA)	θ_{fluct} (°CA)
PI	1028	15.1	1.8
ADRC	814	13.8	0.8
HDRC	494	12.3	0.6

$$DuCy_{Holding} = DuCy_{Holding} + HoldingCyl_{cor} \tag{17}$$

where α and β can be calibrated to tune the compensation speed.

This algorithm is disabled when the valve timing goes into a small error band to avoid the small oscillations caused by the algorithm.

4. Experimental validation

Experimental validations of HDRC were carried out on the VVT control test bed mentioned in Section 2.4, in order to test its robustness to variations of oil pressure and engine speed, and the disturbance rejection ability to the fast oil pressure fluctuation. Three evaluation indexes were proposed to quantify the control performance, including the settling time (in this paper, defined as the time duration between the moment when the valve timing order is sent and the moment after which the valve timing error stays ± 5 °CA, denoted as T_s), the integral time absolute error (*ITAE*), as well as the fluctuation amplitude in steady state (θ_{fluct}).

First, as a baseline, the control performance comparison of three controllers, the manually tuned PI controller and ADRC controller as well as the HDRC controller, was carried out at 1200 rpm, 3.5 bar oil pressure and 40 °C oil temperature (the oil temperature is all around 40 °C in this paper), with the valve timing stepping from 50 °CA to 10 °CA as shown in Figs. 9 and 10, results of which are summarized in Table 1. It can be noticed that ADRC has obvious advantage over PI in terms of faster response (about 21% improvement) and accurate tracking performance (about 56% improvement). With FF, the response speed can be further improved (to about 51.9% compared with PI) as analyzed in Section 3.3 but, the tracking precision stays almost the same since FF was disabled in the steady state condition. For the purpose of evaluating the effect of ADRC and FF as a whole, HDRC was systematically compared with a pure PI controller in Sections 4.1 and 4.2, at different operating conditions and in face of oil pressure fluctuations, without gain-scheduling for neither of them.

4.1. Robustness test

Variations of the engine speed and oil pressure, common phenomena in practical engines, can change the sampling rate and the system dynamics significantly. It is, therefore, essential to be robust to these variations for realizable VVT control. So, the HDRC and PI controller were tested at low engine speed (800 r/min, in Fig. 11) and low oil pressure (2.0 bar, in Fig. 12) respectively, in

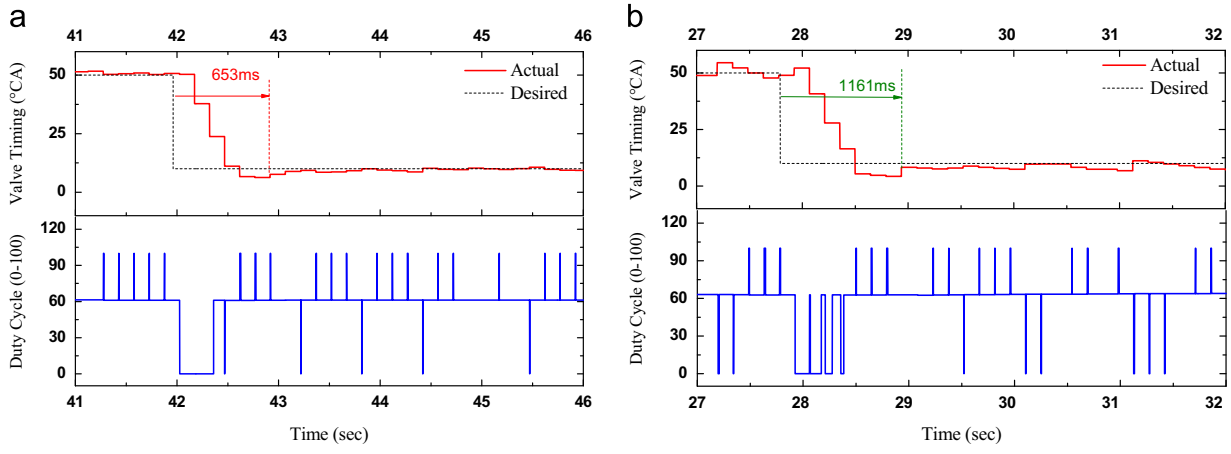

Fig. 11. Control performance comparison between PI and HDRC with 50–10 °CA step at 800 rpm engine speed and 3.5 bar oil pressure, (a) HDRC controller and (b) PI controller.

Please cite this article as: Xie H, et al. A hybrid disturbance rejection control solution for variable valve timing system of gasoline engines. ISA Transactions (2013), http://dx.doi.org/10.1016/j.isatra.2013.10.006

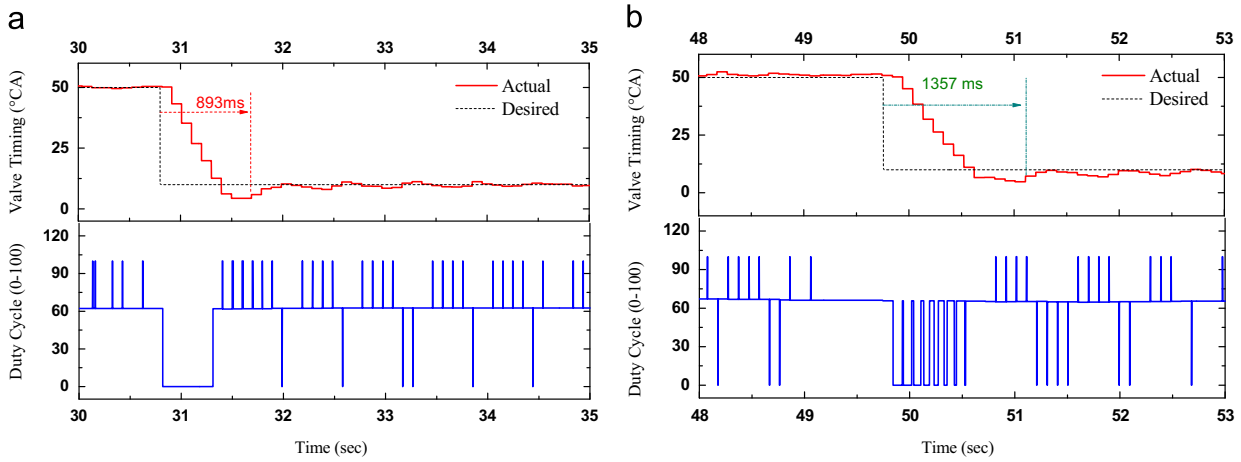

Fig. 12. Control performance comparison between PI and HDRC with 50–10 °CA step at 1200 rpm engine speed 2.0 bar oil pressure profile. (a) HDRC controller and (b) PI controller.

Table 2
Robustness validation of PI and HDRC at different operating conditions.

Operating conditions	PI			HDRC			Improvement of HDCR		
	T_s (ms)	*ITAE* (°CA)	θ_{fluct} (°CA)	T_s (ms)	*ITAE* (°CA)	θ_{fluct} (°CA)	T_s (%)	*ITAE* (%)	θ_{fluct} (%)
1200 r/min 3.5 bar oil pressure	1028	15.1	1.8	494	12.3	0.6	51.9	18.5	27.7
800 r/min 3.5 bar oil pressure	1161	21.4	4.4	503	14.7	1.4	56.6	31.3	68.1
1200 r/min 2 bar oil pressure	1357	21.1	2.5	893	14.6	1.3	31.2	30.8	48

order to test the robustness of HDRC through comparisons as summarized in Table 2.

First, at 800 r/min engine speed condition, the performance of the PI controller was deteriorated notably (see the data in the first two rows in Table 2). This is because the system dynamic changed at the low engine speed, such as the low frequency inverse force from the valve spring, and the control bandwidth was much smaller resulting from the low sampling rate, making the controller parameters inappropriate. However, both the response speed and tracking accuracy of HDRC were well maintained even though the sampling rate, the LESO bandwidth are much lower than that of the baseline (1200 r/min), achieving 56.6% improvement in T_s, 31.3% improvement in *ITAE*, and 61.8% improvement in θ_{fluct} compared with PI.

Second, in the low oil pressure case, the response speed of the two controllers both decrease. This phenomenon is understandable, as lower oil pressure results in smaller driving force of the cam phaser at the same solenoid position. In other words, b_0 was reduced significantly as shown in Eq. (9) leading to varied system dynamics. The performance of PI controller goes worse notably without gain-scheduling. However, HDRC was much less influenced in comparison, with 31.2% improvement in T_s, 30.8% improvement in *ITAE*, and 48% improvement in θ_{fluct} compared with that of PI. Part of the cause lies in the FF controller for the driving-stage signal compensation. What is more, ADRC also contributes a lot to the high robustness, as the b_0 uncertainty has been observed by the LESO and mitigated by the controller.

In order to validate the analysis above and analyze the causes of the robustness intuitively (see Fig. 13), disturbances, estimated by LESO, were compared in the two test cases and the baseline above. Results show that the estimated disturbance varies when the engine speed or oil pressure and engine speed changes, indicating that the system can be made invariant to some extent, i.e., to behave like the canonical system (integral system) in the face of system dynamic changing, through the disturbance estimation and compensation.

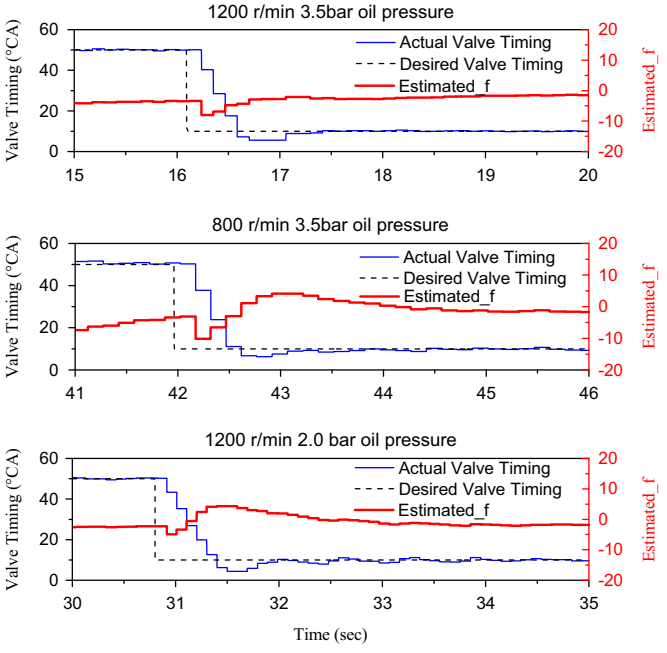

Fig. 13. Intuitive analysis of causes of the high robustness of HDRC.

4.2. Disturbance rejection ability test

Fast fluctuations of oil pressure, caused by the strong variations of engine speed and oil temperature in vehicles, are quite common

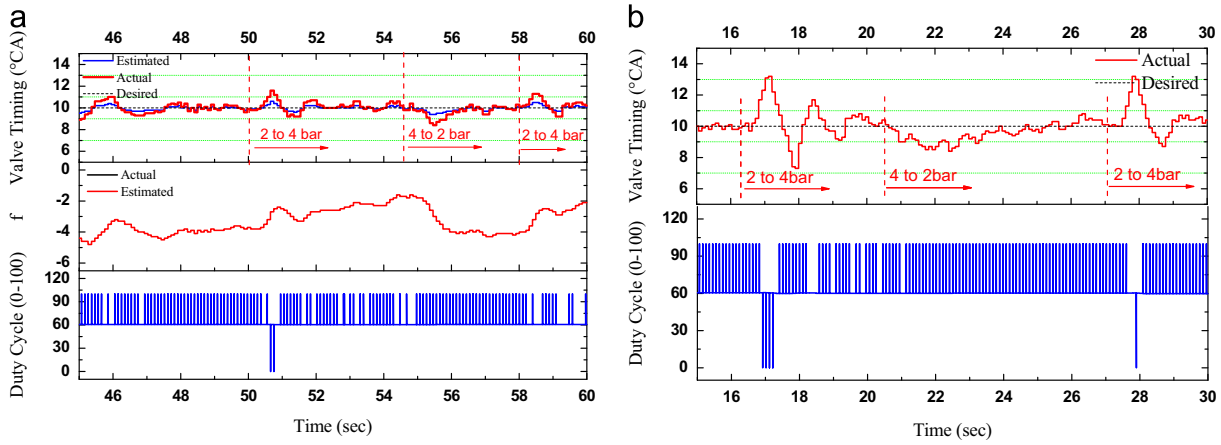

Fig. 14. Disturbance rejection ability to oil pressure variation comparison between (a) HDRC and (b) PI.

Table 3
Disturbance rejection ability comparison between PI and HDRC.

Oil pressure step (bar)	PI		HDRC		Improvement of HDCR	
	ITAE (°CA)	θ_{fluct} (°CA)	*ITAE* (°CA)	θ_{fluct} (°CA)	*ITAE* (%)	θ_{fluct} (%)
2–4	3.3	5.9	1.3	2	60.6	66.1
4–2	2.7	2	1.4	2	48.1	0

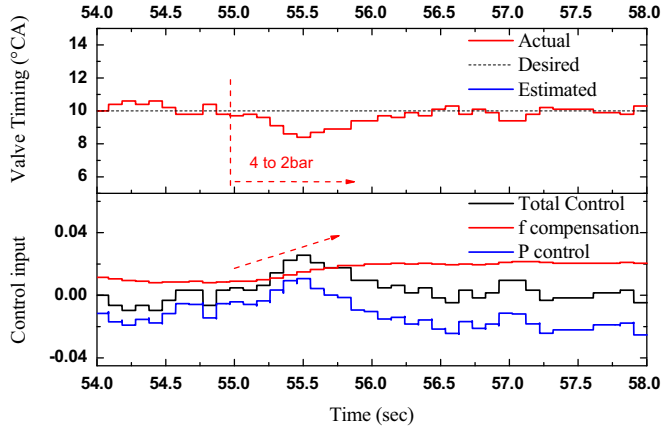

Fig. 15. Causes analysis for high disturbance rejection performance.

in practice, acting as strong disturbances to the control system. Therefore, high disturbance rejection ability is also of importance for realizable VVT control.

So, both PI and HDRC were tested under oil pressure fluctuation conditions, as shown in Fig. 14. The *ITAE* and θ_{fluct} within the 3 s time window after each oil pressure step are summarized in Table 3. For the PI controller, the valve timing was disturbed notably, as the control input is not large enough until apparent valve timing deviation occurs. In comparison, HDRC was less affected with over 48% improvement in *ITAE*, confirming its effectiveness in disturbance rejection.

To analyze the causes intuitively, the control inputs resulting from the proportional control, from f compensation, and from the total control input are illustrated in Fig. 15 in the time window from 54 s to 58 s. Here the total control input element is $-z_2/b_0+K_p/b_0(r-z_1)$, the f compensation element is $-z_2/b_0$, and the proportional control input element is $K_p/b_0(r-z_1)$. It can be intuitively noticed that the dynamic variation due to the oil pressure step is observed by HDRC through the f estimation, compensated on time through the f compensation element, making the system always behave like the canonical model.

5. Concluding remarks

In this paper, the HDRC strategy for the hydraulic–magnetic VVT system control is proposed. The influence of the oil pressure and temperature on the VVT response behavior is captured using a simple static model, based on which a feed-forward controller was designed to ensure fast response. All the remaining uncertainties and dynamics that are too difficult to model were regarded as disturbances. They were estimated and canceled in real-time by a first-order LADRC controller, demonstrating a simple but effective disturbance rejection ability. HDRC was validated and compared with an existing manually tuned PI controller in several experiments demonstrating a remarkable advantage in response speed and robustness to oil pressure and engine speed variations. Likewise, the disturbance rejection ability is also shown, using the timely disturbance compensation of ADRC, making it a promising candidate among competing solutions for VVT control.

Acknowledgments

This study was supported by Project of National Nature Science Foundation of China (Grant no. 51376135) from National Nature Science Foundation Committee of China.

The authors also want to show great thanks to Prof. Zhiqiang Gao, Qinling Zheng and Jason Tatsumi from Cleveland State University for their valuable suggestions and help.

References

[1] Fontana G, Galloni E. Variable valve timing for fuel economy improvement in a small spark-ignition engine. Appl Energ 2009;86(1):96–105.
[2] Zhao H, Li J, Ma T, Ladommatos N. Performance and analysis of a 4-stroke multi-cylinder gasoline engine with CAI combustion. SAE world congress. Detroit, US; April 2002, 2002-01-0420.
[3] Xie H, Hou S, Qin J, Zhang Y., Li N. Control strategies for steady and transient operation of a 4-stroke gasoline engine with CAI combustion using a 4-variable valve actuating system (4VVAS). SAE world congress. Detroit, US; April 2006, 2006-01-1083.
[4] Ekdahl E, Taylor R. VCT solenoid dither frequency control. United States patent, US6736094 [18.5.2000].
[5] Doi T, Sato O, Yamaguchi J, Hori A. Variable valve timing control apparatus for an internal combustion engine. United States patent, US6135078 [24.10.2000].

[6] Kondou S, Koyama H. Valve control apparatus and method for internal combustion engine. United States patent, US6755165 [29.6.04].
[7] Tao J, Li L, Chang W, Xiao M. The variable valve timing system based on neural network and fuzzy controller. Chin J Sci Instrum 2003;24(3):305–8 (in Chinese).
[8] Lee T, Filipi Z. Nonlinear model predictive control of advanced engines using discretized nonlinear control oriented models. SAE word congress. Detroit, US; April 2010, 2010-01-2216.
[9] Corvino C, Calabretta M, Zanasi R. Modeling of variable valve timing on high performance engine using power-oriented graphs method. SAE word congress. Detroit, US; 2011, 2011-24-0150.
[10] Gao Z, Huang Y, Han J. An alternative paradigm for control system design. Proc IEEE Conf Decis Control 2001;5:4578–85.
[11] Han J. From PID to active disturbance rejection control. IEEE Trans Ind Inf 2009;56(3):900–6.
[12] Gao Z. Active disturbance rejection control: a paradigm shift in feedback control system design. In: Proceedings of the American control conference. Minneapolis, MN; June 2006, p. 2399–405.
[13] Zheng Q, Chen Z, Gao Z. A practical approach to disturbance decoupling control. Control Eng Pract 2009;17(9):1016–25.
[14] Goforth JF, Zheng Q, Gao Z. A novel practical control approach for rate independent hysteretic systems. ISA Trans 2012;51(3):477–84.
[15] Dong L, Zhang Y, Gao Z. A robust decentralized load frequency controller for interconnected power systems. ISA Trans 2012;51(3):410–9.
[16] Kotina R, Zheng Q, Antonie Bogert J, Gao Z Active disturbance rejection control for human postural sway. In: Proceedings of the American control conference. San Francisco, CA; June, 2011, p. 4081–6.
[17] Gao Z. Scaling and bandwidth-parameterization based controller tuning. In: Proceeding of the American control conference. Denver, CO, vol. 6; June 2003, p. 4989–96.
[18] Zhao S. Practical solutions to the non-minimum phase and vibration problems under the disturbance rejection paradigm [Ph.D. dissertation]. Cleveland, OH: Cleveland State University; 2012.
[19] He Y. Research on variable valve timing system control of gasoline engine based on active disturbance observation [Master dissertation]. Tianjin, China: Tianjin University; 2012.

Please cite this article as: Xie H, et al. A hybrid disturbance rejection control solution for variable valve timing system of gasoline engines. ISA Transactions (2013), http://dx.doi.org/10.1016/j.isatra.2013.10.006